Available online at www.sciencedirect.com
SCIENCE DIRECT
Journal of Inorganic Biochemistry 93 (2003) 71–83
Journal of Inorganic Biochemistry
www.elsevier.com/locate/jinorgbio

Proton-coupled electron transfer in Fe-superoxide dismutase and Mn-superoxide dismutase

Anne-Frances Miller[a,b,c,*], K. Padmakumar[a], David L. Sorkin[b], A. Karapetian[a], Carrie K. Vance[c]

[a] *Departments of Chemistry and Biochemistry, University of Kentucky, Rose Street, Lexington, KY 40506-0055, USA*
[b] *Department of Chemistry, The Johns Hopkins University, Baltimore, MD 21218, USA*
[c] *Jenkins Department of Biophysics, The Johns Hopkins University, Baltimore, MD 21218, USA*

Received 25 April 2002; received in revised form 20 November 2002; accepted 20 November 2002

Abstract

Fe-containing superoxide dismutase (FeSOD) and MnSOD are widely assumed to employ the same catalytic mechanism. However this has not been completely tested. In 1985, Bull and Fee showed that FeSOD took up a proton upon reduction [J. Am. Chem. Soc. 107 (1985) 3295]. We now demonstrate that MnSOD incorporates the same crucial coupling between electron transfer and proton transfer. The redox-coupled H^+ acceptor has been presumed to be the coordinated solvent molecule, in both FeSOD and MnSOD, however this is very difficult to test experimentally. We have now examined the most plausible alternative: that Tyr34 accepts a proton upon SOD reduction. We report specific incorporation of ^{13}C in the C^{ζ} positions of Tyr residues, assignment of the C^{ζ} signal of Tyr34 in each of oxidized FeSOD and MnSOD, and direct NMR observations showing that in both cases, Tyr34 is in the neutral protonated state. Thus Tyr34 cannot accept a proton upon SOD reduction, and coordinated solvent is concluded to be the redox-coupled H^+ acceptor instead, in both FeSOD and MnSOD. We have also confirmed by direct ^{13}C observation that the p*K* of 8.5 of reduced FeSOD corresponds to deprotonation of Tyr34. This work thus provides experimental proof of important commonalities between the detailed mechanisms of FeSOD and MnSOD.

Keywords: Superoxide dismutase; Proton-coupled electron transfer; FeSOD; MnSOD

1. In the spirit of Professor W. H. Orme-Johnson

How doth the protein big and slow
control whence electrons come and go?
How do they tame these tiny sparks,
entrain them to make bonds and work?

For though electrons move with speed
and quantum mechanical particles be
their charge engenders long-range forces
which when applied to sinks and sources
determine from which bond they'll go
and to which product they will flow.

While in metal-orbitals d
electrons from each other flee,
yet their final destinations
depend thermodynamically on proton locations

Thus, exploiting exquisite control
of labile protons, enzymes cajole
electrons to go or stay
and so a specific product make.

In superoxide dismutase
whose activity extends our days
electrons shuttle to and fro.
One from superoxide to metal goes.
The metal is then reoxidized
as an electron to O_2^- flies.

How can reducing $O_2^{-\cdot}$ oxidize?
Because protons mobilize.
Initial, reduction of active site iron
is coupled to uptake of a proton

$$O_2^{-\cdot} + H^+ + Ez(Fe^{3+}) \rightarrow O_2 + EzH^+(Fe^{2+}) \quad (1a)$$

*Corresponding author. Tel.: +1-859-257-9349; fax: +1-859-323-1069.
E-mail address: afm@pop.uky.edu (A.-F. Miller).

0162-0134/02/$ – see front matter
doi:10.1016/S0162-0134(02)00621-9

Then, so O_2^- will accept an electron
the protein foists on it a proton.

$$O_2^{-\cdot} + EzH^+(Fe^{2+}) + H^+ \rightarrow H_2O_2 + Ez(Fe^{2+}) \quad (1b)$$

where Ez is the entire enzyme
that hosts the protons that move each time.

What are these protons' identities
and their p*K*s, their energies?
How are their coming and their going
coupled to electron storing?

We show here that in FeSOD,
to Fe^{3+}-hydroxide a proton is bound
upon reduction of the Fe center,
so bound hydroxide becomes water

$$e^- + H^+ + L_4Fe^{3+}OH^- \rightarrow L_4Fe^{2+}H_2O \quad (2)$$

When substrate, Fe^{3+} regenerates,
this water, substrate protonates.
This is a proposal of long-standing,
but our data provide new grounding
by showing that nearby tyrosine
does not participate in this scheme.

In MnSOD the same's assumed.
But herein 'tis finally proved
that along with Mn^{3+} reduction
the MnSOD enzyme acquires a proton.

Thus the enzyme can provide
Hs for product peroxide,
and by turning their p*K*s
make electrons go or stay.

So, by protons, electrons are led
whether to metal or substrate instead,
and proteins acquire adept control
via protons, in part or whole
in networks, and with p*K*s set
by the protein environment.

To your ebullient spirit, Bill,
Anne-Frances Miller (P.D.)

2. Introduction

The Fe- and Mn-containing superoxide dismutases (SODs) catalyze the disproportionation of superoxide to hydrogen peroxide and dioxygen, and thus forestall superoxide-initiated oxidative damage [1–3]. The mechanism involves alternating reduction and oxidation of the catalytic metal ion [4], whose reduction midpoint potential (E_m) must therefore be tuned to a value intermediate between those describing oxidation of $O_2^{\cdot -}$ and reduction of $(O_2^{\cdot -} + 2H^+)$ [5,6]. Thus,

$$O_2^{-\cdot} + H^+ + Ez(M^{3+}) \rightarrow O_2 + EzH^+(M^{2+}) \quad (3a)$$

$$O_2^{-\cdot} + EzH^+(M^{2+}) + H^+ \rightarrow H_2O_2 + Ez(M^{3+}) \quad (3b)$$

where M signifies the metal ion and Ez indicates all the rest of the enzyme, including all the metal ion ligands.

Two protons must be supplied to substrate to generate product. Electron transfer to $O_2^{\cdot -}$ is inherently unfavourable because $O_2^{\cdot -}$ is already negatively charged and because the LUMO is an antibonding orbital, so protonation is most likely to be a pre- or co-requisite for reduction of $O_2^{\cdot -}$ [7,8]. Transfer of the second proton has been proposed to be the rate-limiting step [9,10], and the second proton may aid in product dissociation by displacing bound metal ion from nascent product, in an inner-sphere mechanism [9]. FeSOD has been shown to take up one proton upon reduction, throughout the pH range of activity (Eq. (3a) [9]). The redox-coupled proton is therefore rereleased upon metal ion oxidation (Eq. (3b)) and becomes available locally as substrate becomes reduced. Thus, reduction of substrate can be thought of as proton-coupled electron transfer (PCET, [11,12]). The corollary is that reduction of the enzyme is also PCET, and the reduction midpoint potential of the enzyme becomes a function not only of the intrinsic reduction potential of the metal ion, but also of the oxidized and reduced state p*K*s, pK_{ox}^{redox} and pK_{red}^{redox}, of the group that takes up a proton upon metal ion reduction: the redox-coupled proton acceptor [13–15]. Thus,

$$E_m(pH) = E_{AH} + \frac{RT}{F}\ln\frac{K_{red}^{redox} + [H^+]}{K_{ox}^{redox} + [H^+]} \quad (4)$$

where E_{AH} is the reduction potential the enzyme would have at a low pH at which it is fully protonated in both oxidation states (Scheme 1).

Thus, in order to understand the mechanism of SOD, it is necessary to know the identity of the redox-coupled proton acceptor (redox-coupled H^+ acceptor, RCHA), since this group is almost certainly the source of one of the

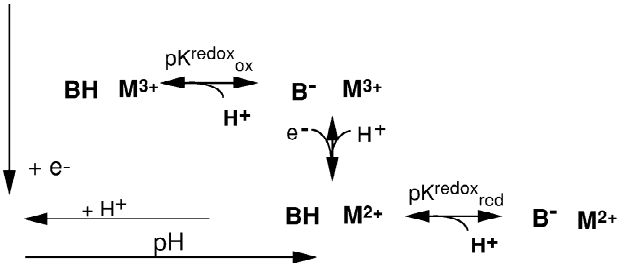

Scheme 1. Proton uptake coupled to reduction, and the relationship between pK_{ox}^{redox} and pK_{red}^{redox}, the p*K*s of the RCHA (here denoted by B), in the presence of the oxidized and reduced states of the metal ion M.

two protons acquired by the product H_2O_2, and this group will play a crucial role in redox tuning. This group has been most reasonably proposed to be the coordinated solvent ligand [16] based on arguments that the metal centre's charge should be minimized since it is buried inside a (low dielectric) protein, and consistent with the tight coupling between coordinated solvent p*K*s and metal ion oxidation state [17].

However, this identity has not been proven experimentally. Moreover, PCET has only been demonstrated for FeSOD, not MnSOD. This is too fundamental an element of the mechanism to accept without experimental support, especially since emerging evidence indicates that the active site ionization events in MnSOD are not the same as those in FeSOD [18,19]. This and the fact that MnSOD forms an inactive intermediate not formed in substantial quantity by FeSOD [4,20,21], call into question the prevailing practice of assuming the same detailed mechanism for MnSOD as has been shown for FeSOD. Thus, with the current work we are finally able to replace the optimistic speculations of the past 15 years with experimental evidence showing that MnSOD does indeed take up an H^+ upon reduction and thus can exploit PCET in the dismutation of $O_2^{\cdot-}$.

The active site metal ion of FeSOD and MnSOD is coordinated in a trigonal bipyramid by three His, one Asp^- and a molecule of coordinated solvent, as shown in Fig. 1 [22]. The axial ligands are His26 and the coordinated solvent, which shares a hydrogen bond with the ligand Asp^- and another with the conserved active site Gln. The Gln, in turn hydrogen bonds to three other protein residues, deriving from both domains of the protein, and thus serves to couple the coordinated solvent to the rest of the protein matrix. All three hydrogen bonding partners are conserved in FeSODs and MnSODs, and the universally-conserved Tyr34 is of particular interest here because it contributes to the p*K* of 8.5–9.7 affecting catalytic activity [16,18,19,22–29].

The oxidized state p*K* of Fe^{3+}SOD is known to correspond to an inner-sphere event based on its effect on the optical and EPR signals of Fe^{3+}SOD [30] and is assigned to OH-binding as a sixth ligand, based on EXAFS [31], MCD [18] and X-ray crystallography [32]. Thus, at neutral pH, existing coordinated solvent was implied to be OH^- instead of H_2O, since deprotonation of the latter might be expected to take precedence over OH^- binding. The reduced state (Fe^{2+}SOD) was found to also have a p*K* of 8.5, that is absent when Tyr34 is mutated to Phe [24,25]. Thus at neutral pH, Tyr34 is protonated in the reduced state. Given that one proton is taken up upon reduction below the p*K*s, the two possible options are that Tyr34 is ionized in the oxidized state and becomes protonated upon reduction (coordinated solvent is OH^- in reduced SOD, Scheme 2B), or that Tyr34 is neutral in oxidized FeSOD and coordinated solvent becomes protonated to H_2O upon reduction (Scheme 2A). Protonation of coordinated OH^- is more consistent with model chemistry but proton uptake by Tyr34 remains a possibility given that protein environments can strongly modulate the p*K*s of amino acids in hydrogen bond networks and Tyr34 is close to the net positively charged metal centre. In order to distinguish experimentally between these possibilities it is necessary to

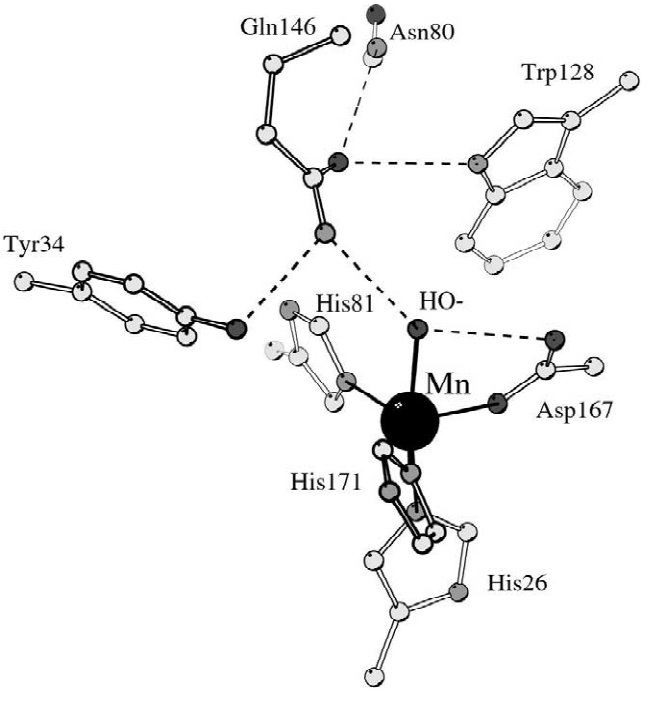

Fig. 1. Cartoon of the active site of MnSOD based on the coordinates of Borgstahl et al. [76]. O atoms are in dark grey, N atoms are in light grey and C atoms are in faintests grey.

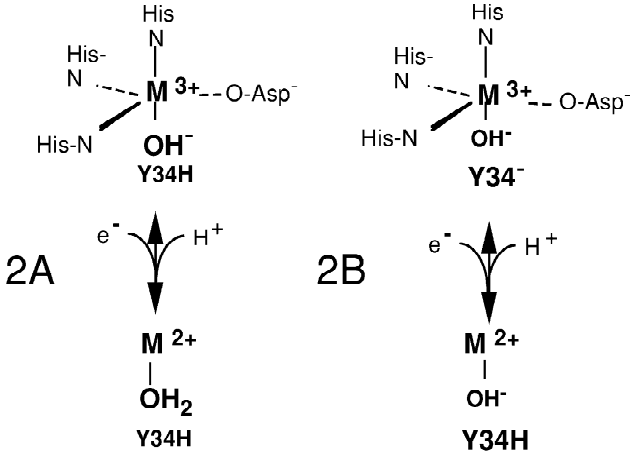

Scheme 2. Alternative possible schemes for proton uptake upon reduction of the SOD active site. In (A), the RCHA would be coordinated solvent whereas in (B), the RCHA would be nearby Tyr34 (Y34). The upper end of each equilibrium includes short-hand notation for the four amino acid ligands to the metal ion (M). These are still present in the reduced state of SOD but are omitted here for simplicity.

know either the protonation state of Tyr34 in Fe^{3+}SOD or that of coordinated solvent in Fe^{2+}SOD.

Protonation states of coordinated solvents are very difficult to ascertain experimentally, however the chemical shift of the C^{ζ} of Tyr changes by 8 ppm upon deprotonation of free Tyr in water. Thus, in the following, we have used ^{13}C NMR spectroscopy to determine the protonation state of Tyr34 in the oxidized states of MnSOD and FeSOD. In addition to confirming the crucial assumption that electron transfer is coupled to proton transfer in MnSOD, our results provide experimental evidence that in both FeSOD and MnSOD, the RCHA is the coordinated solvent (Scheme 2A).

3. Materials and methods

3.1. Proteins

MnSOD was overexpressed from the sodA-, sodB-*E. coli* strain QC774 transformed with the sodA gene on plasmid pDT1-5 [33] or pALS1 [34] and purified as described previously [35,36]. FeSOD was similarly overexpressed in QC774-DE3 from the pET-derived plasmid pRK3 bearing the sodB gene for FeSOD, constructed by Ron Koder, and purified as first described by Slykhouse and Fee [24,37]. Specific activity was determined using the standard xanthine oxidase/cytochrome *c* assay [38]. Protein concentrations were determined using $\varepsilon_{280} = 8660\ M^{-1}\ cm^{-1}$ for MnSOD [39] and $10\,100\ M^{-1}\ cm^{-1}$ for FeSOD [37], respectively. Typical specific activities were 7000 U (mg protein)$^{-1}$ for FeSOD and 6000 U (mg protein)$^{-1}$ for MnSOD.

In order to facilitate observation of the ζ carbon of Tyr side chains, these were selectively labeled with ^{13}C. Bacterial cultures were grown in M9 minimal medium supplemented with 1 g/l glyphosphate to inhibit biosynthesis of aromatic amino acids [40], as well as 50 mg/l Trp, 35 mg/l Phe and 50 mg/l $^{13}C^{\zeta}$-Tyr to support protein synthesis, and overexpression was induced with 1 mM IPTG when A_{600} reached 1. Three hours later, cultures were harvested and the protein purified and manipulated as usual.

3.2. Redox-coupled proton uptake titrations

Visible absorption spectra were collected on a Hewlett Packard 8452A diode array spectrophotometer equipped with a thermostated cell compartment. The extinction coefficient of Mn^{3+}SOD at 478 nm is known for neutral pH [41], but decreases at higher pH [29,42]. Thus, we carried out a pH titration to measure the extinction coefficient at 478 nm as a function of pH for use in measuring the fraction of MnSOD in the oxidized state at a range of pH values.

Measurement of the stoichiometry of proton uptake upon reduction was carried out as described by Bull and Fee [9] at 25 °C in an air-tight 3-ml cuvette blown to the bottom of a three-port anaerobic vessel. MnSOD protein was first dialyzed extensively against deionized water and used at a concentration of 0.6 mM. After degassing by repeated evacuation and equilibration against Ar, the pH of 3 ml of protein solution was adjusted to the desired pH (the reference pH for the measurement), with standardized degassed 5.86 mM KOH. The pH was monitored continuously using a combination pH microelectrode fitted into a 12 gauge stainless steel needle (Microelectrodes Inc.) mounted in one port of the anaerobic vessel. A 10 mM anaerobic stock solution of dithionite was loaded in a gas-tight Hamilton syringe mounted in a second port of the anaerobic vessel. Each experiment was carried out in two steps.

For each experiment, the visible spectrum was collected and the amount of (oxidized) Mn^{3+}SOD calculated using the extinction coefficient at 478 nm appropriate for the pH under study. In step 1, dithionite was added in small (10–20 μl) aliquots and the Mn^{3+}SOD optical signal recorded after each, until MnSOD was almost completely reduced. The pH was returned to the reference pH for the experiment by titration with the standardized KOH, and the change in A_{478} was used to calculate the change in the amount of Mn^{3+}SOD. This was taken as the number of electron equivalents taken up by Mn^{3+}SOD (n_e, in nmol). The volume of KOH added was used to calculate the net number of proton equivalents released ($H_{net,1}$). This includes protons released upon dithionite oxidation (H_{dt}) as well as those associated with impurities (H_x), minus the number taken up by Mn^{3+}SOD upon reduction (H_{SOD}). Since the product of dithionite oxidation is sulfite, which has a pK of 6.9, $2H_2O + S_2O_4^{2-} \rightarrow 2HSO_3^- + 2e^- + 2H^+$, $HSO_3^- \leftrightarrow SO_3^{2-} + H^+$ (pK = 6.9, [9]), the number of protons released per electron derived from dithionite is $(\Delta H/e)_{dt} = 1 + K_A/(K_A + [H^+])$, where K_A is 10^{-pK}. Thus, $H_{net,1} = H_x + n_e(1 + K_A/(K_A + [H^+])) - H_{SOD}$. In order to control for protons released or taken up by (unknown) impurities of the dithionite, a second datum was collected for each experiment.

After MnSOD was fully reduced and the pH was adjusted as necessary to the reference value for the experiment, a volume of dithionite approximately equal to the volume that was used to reduce Mn^{3+}SOD in step 1 was added, in small aliquots as in step 1. The pH was then restored once more to the reference value for the experiment by titration with the standardized KOH. The volume of KOH needed was adjusted for any difference between the volumes of dithionite added in steps 1 and 2, by multiplication by vol_1/vol_2. Thus, in this second step, we measured the net number of proton equivalents released by

the impurities associated with dithionite but apparently without substantial dithionite oxidation[1] and associated proton release, or attendant reduction and protonation (if any) of MnSOD. $H_{net,2}=H_x$. Thus subtraction of $H_{net,2}$ from $H_{net,1}$ allowed us to determine the net number of proton equivalents taken up by MnSOD relatively free of uncertainty due to the unknown purity of the dithionite

$$H_{net,1}-H_{net,2}=n_e\left(1+\frac{K_A}{K_A+[H^+]}\right)-H_{SOD}$$

Upon division by n_e we obtained $H_{SOD}/n_e=\Delta H/e^-$ for MnSOD for the reference pH value of the experiment. The same experiment was repeated for a series of different reference pH values.

3.3. NMR samples and pH titrations

NMR samples contained approximately 30 mg of FeSOD or MnSOD in 0.5–0.6 ml, resulting in dimer concentrations of approximately 1.2 mM. ^2H_2O was included to a final concentration of 10% v/v. Because FeSOD is stabilized at high pH by very low ionic strengths, FeSOD was dialyzed extensively against deionized water prior to pH titrations. For the anaerobic pH titration of Fe^{2+}SOD, a stock solution of NMR pH indicator molecules and 4,4-dimethyl-4-silapentane sodium sulfonate (DSS) was added to Fe^{3+}SOD to produce final concentrations of 2 mM imidazole, 1 mM 2,4-dimethyl imidazole, 0.3 mM trimethylamine, 0.3 mM dimethylamine and 0.3 mM DSS [24]. Samples were then degassed in an NMR tube and reduced with a 1.3× molar ratio of similarly degassed dithionite solution. One reference sample of Fe^{2+}SOD contained 10 mM NaCl, 10 mM morpholinoethanesulfonic acid (MES) at pH 6.0 and 0.2 mM DSS, to permit direct calibration of the ^{13}C chemical shift axis.

The pH of the Fe^{2+}SOD sample was determined at each point in the titration based on the highly pH-sensitive chemical shifts of the pH indicator molecules included in the sample [24,43,44]. Fe^{2+}SOD's pH was titrated by repeatedly cutting open the sample tube in an Ar-filled glove bag, adding an aliquot of degassed 100 mM KOH, mixing gently, sealing temporarily with a septum and then flame sealing upon removal from the glove bag. The NMR line widths of the pH indicator molecules were used to ascertain that a uniform pH had been achieved throughout the NMR sample. A total of three NMR spectra were obtained at each pH point: the ^{1}H spin-echo spectrum used to observe the pH indicators, a conventional ^{13}C spectrum of all Tyr side chains and a saturating ^{13}C spectrum to selectively observe the paramagnetically relaxed resonance of Tyr34 (below). Fe^{3+}SOD and Mn^{3+}SOD samples were adjusted to the desired pH using KOH prior to loading in the NMR tube.

3.4. NMR conditions

Data were collected on a 500 MHz Unity^{plus} or 600 MHz Inova spectrometer equipped with a 5 mm probehead, at 125 MHz or 150 MHz for ^{13}C, respectively. Spectra were collected at 30 °C for FeSOD and 25 °C for MnSOD. All chemical shifts were referenced to internal DSS at 0 ppm [45] and under our conditions, the $^{13}C^{\zeta}$ chemical shifts for free Tyr in water were 157.6 ppm when protonated, 165.8 ppM when ionized. The ^{1}H resonances of internal pH indicators [24] were measured using a spin echo pulse sequence incorporating 30 ms delays to allow for complete relaxation of protein resonances. ^{13}C resonances of SOD were detected non-selectively using a 30° observe pulse, 1 s acquisition and 1 s relaxation delay with WALTZ [46] decoupling of ^{1}H applied throughout. The transmitter offset was set to 140 ppm in order to afford good excitation of $^{13}C^{\zeta}$, while avoiding a center-band artifact in the spectral region of most interest. The side chain C of Tyr34 was observed selectively on the basis of its shorter T_1 resulting from its closer proximity to Fe or Mn than any other Tyr C^{ζ}. Thus, all Tyr C^{ζ} resonances were saturated by WALTZ [46] or WET [47,48] presaturation or inverted with a 180° pulse (the superWEFT method [49]), and then a short delay was allowed for instrument stabilization and recovery of a substantial fraction of Tyr34 magnetization, prior to observation using a 90° pulse. The combination of saturation or inversion, short relaxation time and short recycle time effectively suppresses the resonances of Tyr C^{ζ}s not paramagnetically relaxed by Fe^{2+}, Fe^{3+} or Mn^{3+}. Spectra were processed with Lorentz or Gaussian line broadening as indicated in the figure captions.

4. Results

4.1. Proton coupled electron transfer

Bull and Fee showed that FeSOD takes up one proton in conjunction with one electron, across the whole pH range of activity [9]. However, the same has not previously been demonstrated for MnSOD. Fig. 2 shows the course of MnSOD reduction by dithionite at pH 9.64 and the points in the titration at which the pH was restored to 9.64 (steps 1 and 2, see Methods section).

[1]Optical spectra collected after the second series of dithionite additions show that the signal of dithionite increases, and thus that dithionite accumulates rather than reacting with some species, becoming oxidized and releasing protons. We also confirmed that sulfite was not able to reduce Mn^{3+}SOD at the concentrations used in these experiments. Thus, we do not invoke the oxidation of sulfite to sulfate with attendant release of another proton per electron.

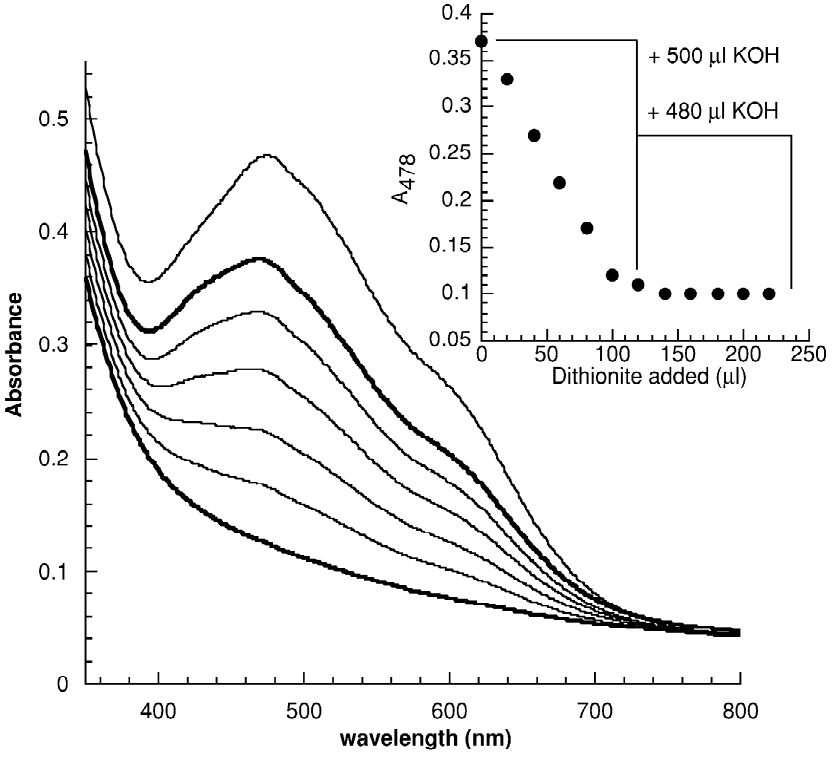

Fig. 2. Measurement of the number of protons taken up in conjunction with reduction of Mn^{3+}SOD, at pH 9.64. The optical spectrum of the Mn^{3+}SOD remaining is shown at various points in its stepwise reduction by 500 µl of dithionite. When MnSOD reduction, as indicated by the A_{478}, was virtually complete, the pH was returned to 9.64 by addition of 500 µl of KOH. The pH was adjusted back to 9.64 a second time after addition of 100 µl more dithionite, in order to determine the amount of base required to compensate for the effects of impurities in the dithionite, in the absence of a reaction between dithionite and MnSOD (after multiplication by 1.2 to account for the different volumes of dithionite added in step 1 and 2). Thus, the number of proton equivalents released in the course of reduction of MnSOD by dithionite could be determined, as described further in the Methods section.

The same experiment was repeated at a series of pH values and the pH profile of $\Delta H^+/e^-$ is plotted in Fig. 3. Throughout the pH range of MnSOD activity, electron acceptance is coupled to proton uptake, as in FeSOD. However in the pH range of 8.6 to 11.1, $\Delta H^+/e^-$ is significantly larger than below pH 7.6, with a maximum of 1.9 proton equivalents taken up upon reduction at pH 9.6. Thus, the active site contains more than one H^+ acceptor and must be described by at least two p*K*s in each of the oxidized and reduced states. In addition to the RCHA, there must be another group that becomes (or is replaced by) a stronger base in the reduced state than in the oxidized state. The effect of a second pair of p*K*s on $\Delta H^+/e^-$ is described by Eq. (5), in which K_{ox} and K_{red} are the acid dissociation constants pertaining to the second group in the oxidized and reduced state, respectively, corresponding to the observed p*K*s, pK_{ox} and pK_{red}, and the contribution of the RCHA is incorporated as the 1 at the beginning of the right side of the equation

$$\Delta H^+/e^- = 1 + \left(1 + \frac{K_{red}}{[H^+]}\right)^{-1} - \left(1 + \frac{K_{ox}}{[H^+]}\right)^{-1} \qquad (5)$$

This equation, using $pK_{ox} = 8.7 \pm 0.1$ and $pK_{red} = 11.8 \pm 0.1$, describes our data well ($R = 0.99$).

4.2. Identity of the redox-coupled proton acceptor

The two principal candidates for the role of RCHA are Tyr34 and coordinated solvent. Since it is very difficult to unambiguously determine the protonation state of solvent coordinated to metal ions in proteins, we have determined the protonation state of Tyr34 in each of the oxidized and reduced states of FeSOD and in the oxidized state of MnSOD. Beginning with Fe^{2+}SOD, we first establish the assignment of the C^ζ resonance of Tyr34, demonstrate the confidence with which the protonation state of Tyr can be determined based on the $^{13}C^\zeta$ chemical shift and then determine the protonation state of Tyr34 at neutral pH.

The ^{13}C NMR spectrum of SOD incorporating $^{13}C^\zeta$-labelled Tyr is highly enriched in ^{13}C at the C^ζ positions of Tyr residues (154–162 ppm), yet the label clearly does not migrate to other positions in significant amounts (Fig. 4). Thus, Tyr C^ζs are relatively easily observed by direct ^{13}C detection and can be identified in selectively labelled protein by their much stronger-than-background signal intensities as well as their characteristic chemical shifts. Direct ^{13}C detection offers the important advantage of permitting observation of even strongly relaxed resonances of residues near the paramagnetic active site metal ion [50,51].

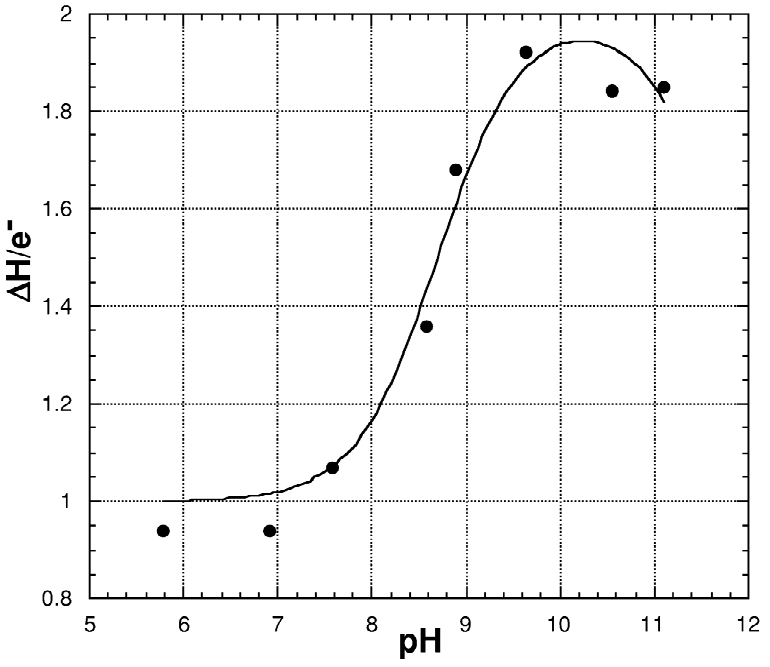

Fig. 3. The number of protons taken up per one-electron reduction of MnSOD ($\Delta H^+/e^-$), as a function of pH. The data were fit with Eq. (5) yielding $pK_{ox} = 8.7 \pm 0.1$ and $pK_{red} = 11.8 \pm 0.1$ with $R = 0.99$.

For Fe^{2+}SOD, deconvolution of the overlapped signal intensity in the Tyr C^{ζ} region reveals nine resonances, consistent with the nine Tyr residues in FeSOD. One of the resonances (at 158.3 ppm) is twice as broad as the others (Fig. 5, top). This resonance also displays the shortest T_1, by approximately a factor of two (Fig. 5, bottom). Thus, it is assigned to the C^{ζ} of Tyr34, which is 5.9 Å from Fe^{2+} [22]. The next closest Tyr C^{ζ} (Tyr76) is 6.5 Å from Fe^{2+}, which under the steep r^{-6} distance dependence of paramagnetic T_2 and T_1 relaxation [52,53] is expected to be almost half as severely relaxed as Tyr34, and could explain the smaller surviving intensity at 159.4 ppm in the superWEFT spectrum of Fig. 5 (bottom). All other Tyrs are more than 8.4 Å away so their line widths will not be significantly affected by paramagnetic relaxation.

^{13}C spectra of [Tyr-$^{13}C^{\zeta}$]-Fe^{2+}SOD were collected at a series of closely-spaced pH values, so that the shifts of the non-overlapping resonances could be followed. Tyr34's resonance was observed separately in spectra collected with superWEFT suppression of resonances not subject to accelerated paramagnetic relaxation ('diamagnetic resonances') [49] in order to avoid confusion between it and resonances of other Tyrs. Fig. 6 shows the resulting pH titration curves. The resonance of Tyr34 titrates with a p*K* of 8.4 ± 0.1, and a 9.5 ppm downfield change in chemical shift which is similar to the 8 ppm downfield change displayed by free Tyr in water. However, the diamagnetic Tyr resonances display much smaller sensitivities to pH more consistent with indirect responses. The failure of more Tyr residues to ionize is consistent with the p*K* near 10.5 expected for Tyr and the fact that the Tyrs of FeSOD are largely buried in the protein interior. However, the close agreement between the p*K*s of the diamagnetic Tyrs' responses (p*K* = 8.5, 8.4 and 8.4) and that of Tyr34 suggests that the other Tyrs are responding to deprotonation of Tyr34. Indeed, FeSOD has several Tyr residues near Tyr34 which may reasonably be expected to respond to Tyr34's deprotonation.

Since the chemical shifts are well within the range of 154–160 ppm normally associated with neutral Tyr C^{ζ} [54], Tyr34's chemical shift is only subtly affected by paramagnetism, if at all. Thus, the event responsible for the change in shift is confirmed to be deprotonation of Tyr34 itself, not an event in the metal ion coordination sphere. The chemical shift change associated with the ionization of Tyr34 is +9.5 ppm, and shifts the Tyr resonance to 167.5 ppm, clearly out of the window expected for neutral Tyr, confirming that the ^{13}C NMR chemical shift change is large enough to be a reliable indicator of Tyr protonation state. However, the p*K* of Tyr34 is lower than expected for free Tyr, possibly due to this Tyr's proximity to the net positively charged active site metal centre, and the hydrogen bond Tyr34 appears to accept from Gln69 [22]. The p*K* of 8.4 obtained is in excellent agreement with the value of 8.5 obtained previously based on then-unassigned ^1H resonances [24]. Thus we have now *directly* assigned the reduced state p*K* of Fe^{2+}SOD to Tyr34, and demonstrated that ^{13}C NMR can selectively observe Tyr34 and accurately reveal the protonation state of Tyr residues in FeSOD even within 6 Å of Fe^{2+}.

In Fe^{3+}SOD, the paramagnetic Fe^{3+} is a much more severe nuclear relaxation agent due to its symmetric high

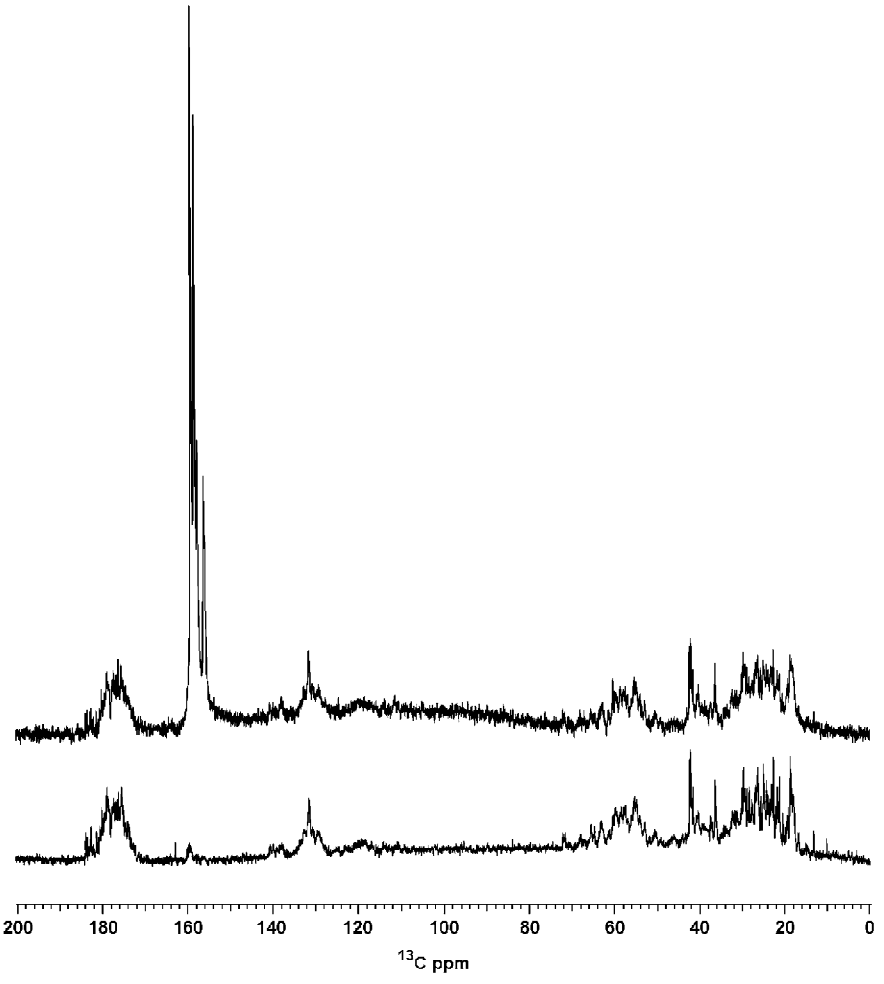

Fig. 4. ^{13}C NMR spectra of Mn^{3+}SOD±selective labelling of Tyr C^{ζ}. Bottom: the natural abundance ^{13}C spectrum of Mn^{3+}SOD and top: Mn^{3+}SOD enriched with ^{13}C at the C^{ζ} position of Tyr residues in addition to ^{13}C at natural abundance at all other sites. Both samples were suspended in 50 mM phosphate buffer at pH 7.5. The greatly enhanced $^{13}C^{\zeta}$ signal intensity near 160 ppm makes the titrations and the saturation experiments possible. Top: 2 s recovery delay, 90° pulse, 1 s acquisition time, 50k scans processed with 5 Hz Lorentzian line broadening; bottom: 1 s recovery delay, 45° pulse, 1 s acquisition time, 32k scans processed with 5 Hz Lorentzian line broadening. Approximate chemical shift ranges for the different protein Cs are: carboxyl and carbonyl Cs between 185 and 170 ppm, Tyr C^{ζ} between 162 and 154 ppm, other aromatic side chain Cs between 130 and 90 ppm, C^{α} between 75 and 45 ppm and other aliphatic Cs between 45 and 10 ppm [74,75].

spin d^5 configuration and thus long electron spin T_1 and T_2 [52,53]. However, by the same token, it is only expected to make paramagnetic contributions to the chemical shifts of ligand nuclei, whereas the chemical shifts of non-ligands, such as Tyr34, are not expected to be altered. Moreover, the relatively normal chemical shifts observed for Tyr34 in Fe^{2+}SOD provide an upper limit to the amount of paramagnetic shifting expected and demonstrate that it will be negligible.

The ^{13}C spectrum of the Tyr C resonances of Fe^{3+}SOD reveals seven resolved resonances (Fig. 7A), consistent with more severe broadening of the resonances of Tyrs nearest to Fe^{3+}: Tyr34 and Tyr76. In order to suppress the sharper and therefore taller resonances of diamagnetic Tyrs, and thus reveal underlying broad resonances, we employed the superWEFT method involving inversion of all magnetization, observation after allowance of only a short recovery period and rapid recycling between scans [49]. Fig. 7 shows that decreasing the intervals allowed for relaxation and recovery suppresses the sharper signals (spectra D and C vs. B and A) and reveals that in addition to the broad signal at 158.6 ppm, there is an even broader feature in the baseline at 159 ppm which persists even when the feature at 158.3 ppm becomes saturated. The very broad intensity is not likely to be residual diamagnetic intensity since the methods used completely eliminate this and leave a flat baseline (Fig. 5, bottom).

The broad resonances account for the two Tyr residues missing from the diamagnetic spectrum. The very broad one is assigned to Tyr34 and the broad one to Tyr76, based on their relative distances from Fe^{3+}SOD (6.0 and 6.5 Å, respectively [22]). While the very broad resonance's

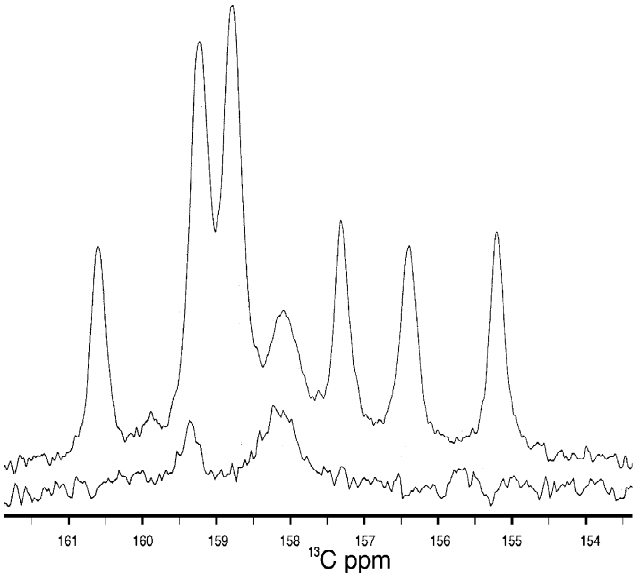

Fig. 5. Expansion of the Tyr C^{ζ} spectral region of Fe^{2+}SOD at pH 7.1, showing five resolved single resonances and two pairs of overlapped resonances for a total of nine Tyr $^{13}C^{\zeta}$ resonances in a normal ^{13}C spectrum (top). In a superWEFT spectrum (bottom) in which diamagnetic ^{13}C resonances are saturated due to short delays between scans and between inversion and observation (see explanation in Results section), the spectrum is dominated by a signal at 158.3 ppm. Top: 1 s recycle delay, 30° pulse, 1 s acquisition time, 16k scans; bottom, 0 ms recycle delay, 180° pulse, 100 ms recovery, 90° pulse, 200 ms acquisition time, 64k scans. Both spectra were acquired at 125 MHz and processed with 5 Hz Lorentzian line broadening.

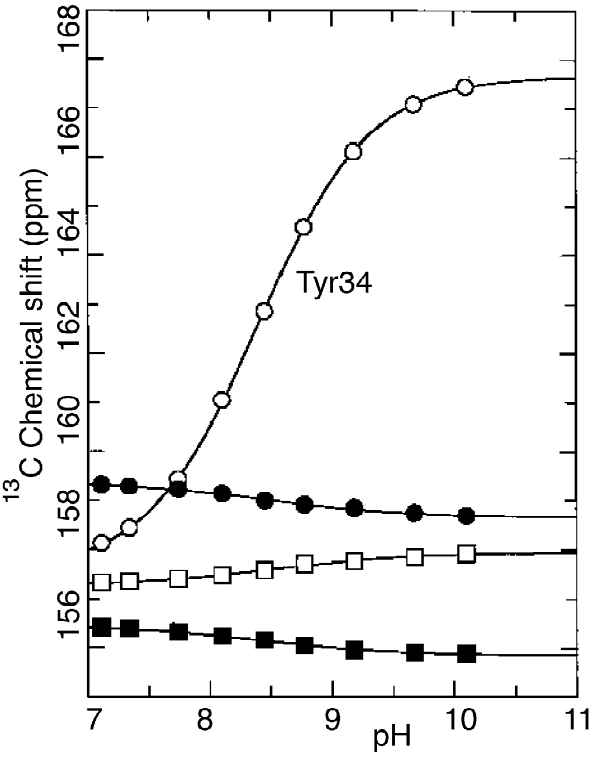

Fig. 6. pH titrations of Tyrs in Fe^{2+}SOD. ○: Tyr34, pK = 8.4±0.1; ●, □, ■: three unassigned resonances described by pKs of 8.53, 8.44 and 8.40±0.1, respectively. The pKs and the curves drawn were obtained from fits to the data of the Henderson–Hasselbalch equation $\delta_A - \delta_{obs}/\delta_A - \delta_B = K/K + 10^{-(pH)}$ where δ_A and δ_B are the chemical shifts of the acid and base forms (the asymptotes obtained from the fit), δ_{obs} is the observed chemical shift at a given pH, K is the acid dissociation constant obtained from the fit and the Hill coefficient is set to 1. The pH dependencies of the unassigned resonances are too small and not of the correct sign to represent deprotonation of the Tyrs to which the resonances correspond. They are most likely to be indirect responses to deprotonation of Tyr34.

chemical shift can only be estimated, as 159±1.5 ppm, both resonances' chemical shifts are in the range expected for protonated Tyr, not the range expected for deprotonated Tyr^-. Moreover even Tyr34's broad line width (≈300 Hz at 125 MHz, or 2.5 ppm) is still significantly smaller than the 8 ppm chemical shift change associated with deprotonation, so it does not obscure the effect. Thus, Tyr34 is found to be protonated in Fe^{3+}SOD at pH 7.5.[2] Moreover, this conclusion holds even if the assignments of Tyr34 and Tyr76 were to be reversed, since both are evidently protonated, based on their chemical shifts. This demonstrates that Tyr34 cannot be the RCHA, thus experimentally confirming coordinated solvent in that role.

In MnSOD, the same residues are present in the active site and Tyr34 has been shown to be protonated at neutral pH in the reduced state [19], so one has the same candidates for the role of RCHA. Again, it is extremely difficult to directly determine the protonation state of coordinated solvent in both oxidation states to test the schemes,[3] so the ionization state of Tyr34 in Mn^{3+}SOD was determined instead. Tyr34 was observed at pH 7.5, where only one group takes up a proton (Fig. 3). Fig. 8 shows the ^{13}C spectrum of the Tyr C^{ζ}s in Mn^{3+}SOD (top). Seven resonances are expected but only six are identified in a deconvolution (yielding two pairs of overlapped resonances and two more resonances). However, presatura-

[2]It was not possible to collect a pH titration of the ^{13}C resonance of Tyr34 in Fe^{3+}SOD, because the degree of paramagnetic line broadening increased dramatically with pH and resulted, at high pH, in it being impossible to reliably localize the centre of the very broad resonance. This increase in line broadening is entirely consistent with the assignment of the oxidized state pK to coordination of OH^- as a sixth ligand [31], as this would complete Fe^{3+}SOD's coordination sphere and increase the symmetry of the unpaired electron spin density, so increasing the expected electron spin T_1 and thus decreasing the T_2 and T_1 of nearby nuclei [52,53].

[3]In MnSOD, the coordinated solvent's identity as OH^- rather than H_2O in the oxidized state is less well established than in FeSOD, although it is consistent with Mn–O distances in the protein crystal structures obtained at 1.8 Å resolution [55] and calculations [56].

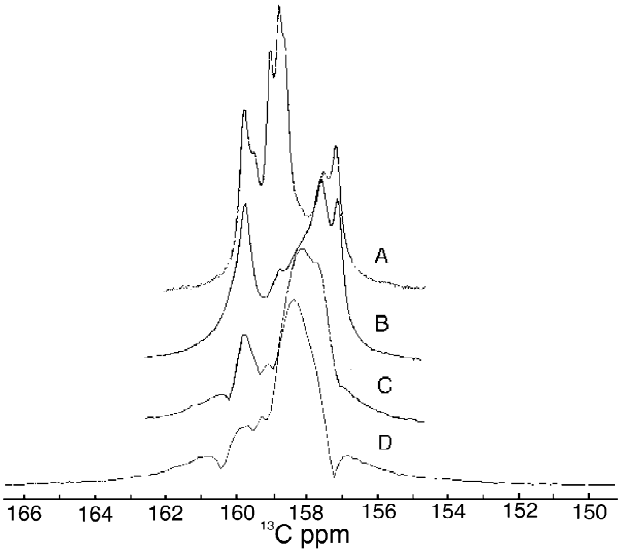

Fig. 7. Increasingly saturated spectra of Fe^{3+}SOD in which saturation of the diamagnetic resonances reveals underlying fast-relaxing paramagnetically broadened resonances. (A) 1 s recycle delay, 90° pulse and 1 s acquisition time, 128k scans; (B) 1 ms recycle delay, 180° pulse, 60 ms recovery, 90° pulse and 100 ms acquisition time, 204.8k scans; (C) 0 ms recycle delay, 180° pulse, 15 ms recovery, 90° pulse and 50 ms acquisition time, 491.5k scans; (D) 0 ms recycle delay, 180° pulse, 10 ms recovery, 90° pulse and 35 ms acquisition time, 655.4k scans. All spectra were acquired at 125 MHz and processed with 1 Hz Lorentzian line broadening.

tion of diamagnetic resonances reveals a broad underlying feature at 159.6 ppm which we assign to Tyr34. This resonance is absent from Y34F $^{13}C^{\zeta}$-labeled Mn^{3+}SOD (Fig. 8, bottom). Moreover, in MnSOD, the C^{ζ} of Tyr34 is 5.9 Å from Mn but the next-closest Tyr (Tyr173) is 8.5 Å away [55], consistent with only one severely broadened Tyr and all other resonances being subject to only approximately one ninth as strong paramagnetic line broadening.

Tyr34's chemical shift of 159.6 ppm is well within the range of 154–160 ppm expected for protonated Tyr, as are the chemical shifts of the other Tyr resonances, and there are no signals in the range of 162–166 ppm expected for Tyr^{-}. Moreover, Tyr34's resonance shifts to 165.5 ppm at high pH, consistent with deprotonation [19]. Thus, Tyr34 is protonated at neutral pH in Mn^{3+}SOD and it cannot accept a proton upon metal ion reduction. Therefore, even without a full titration of Tyr34 it is clear that at neutral pH, Scheme 2B fails for MnSOD, as well as FeSOD, and our data provide experimental support for coordinated solvent as the RCHA.

5. Discussion

Bull and Fee showed that FeSOD takes up one proton upon one-electron reduction [9]. Our determination that reduction of MnSOD is also accompanied by proton

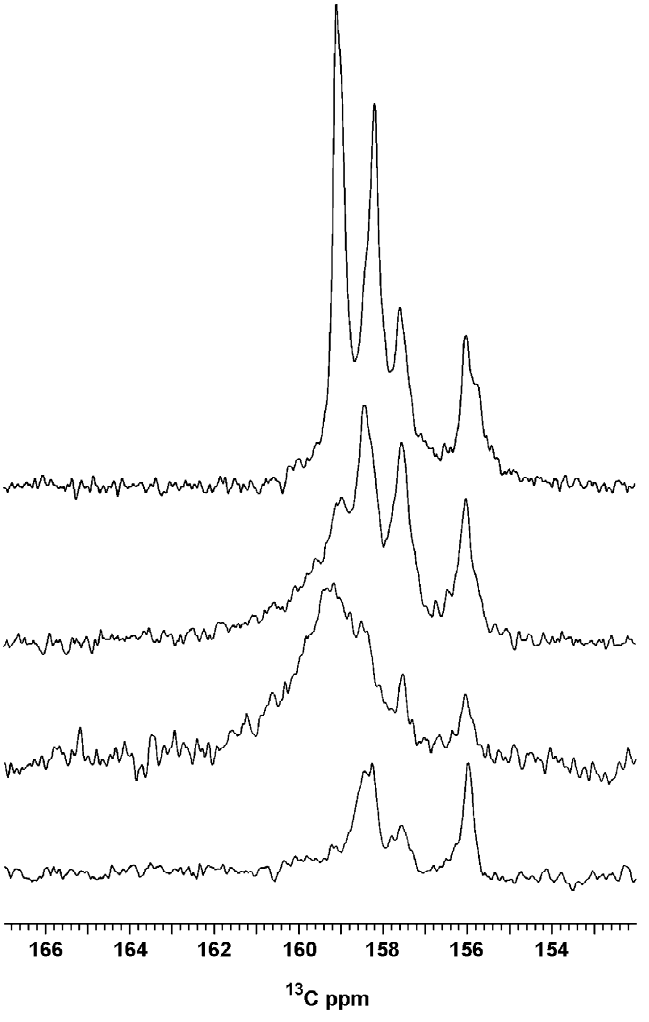

Fig. 8. Increasingly saturated spectra of Mn^{3+}SOD in which saturation of the diamagnetic resonances reveals an underlying fast-relaxing paramagnetically broadened resonance in WT but not Y34F Mn^{3+}SOD. Top, 2 s recycle delay, 30° pulse, 1 s acquisition time, 50k scans processed with 6 Hz Lorentzian line broadening; Second, superWEFT suppression of diamagnetic resonances: 1 ms recycle delay, 180° pulse, 40 ms recovery, 90° pulse and 200 ms acquisition time, 10k scans, processed with 10 Hz Lorentzian line broadening; Third, WET presaturation of all Tyr $^{13}C^{\zeta}$ resonances: 1 ms recovery, 90° pulse, 200 ms acquisition time, 20k scans, processed with 15 Hz Lorentzian line broadening. Bottom, WET presaturaton of all Tyr $^{13}C^{\zeta}$ resonances in Y34F Mn^{3+}SOD; as for third spectrum but with 100 ms acquisition time, 6 Hz Lorentzian line broadening. Bottom, WET presaturation of all Try $^{13}C^{\zeta}$ resonances in Y34F Mn^{3+}SOD; as for third spectrum but with 100 ms acquisition time, 6 Hz Loretzian line broadening. All spectra were acquired at 150 MHz on samples at pH 7.5.

uptake provides crucial support for a similar mechanism as in FeSOD. This is virtually universally assumed but so far experimentally supported primarily by pioneering pulse radiolysis studies [4,20,21]. However, these same studies revealed important differences between the two SODs, in that MnSOD but not FeSOD forms an inactive intermediate [4,20,21]. The very similar active site structures of FeSOD and MnSOD suggest that the two should have similar mechanisms, but small positional differences be-

tween hydrogen bonding partners such as Gln69/146 and Tyr34 could result in significantly different residue p*K*s and thus different roles in proton transfer.[4] Both SODs almost certainly couple protonation of $O_2^{\cdot -}$ to $O_2^{\cdot -}$ reduction, in order to make that reaction thermodynamically accessible and fast enough to be biologically useful. Thus, a proton should be released upon Mn^{2+} oxidation and, consequently, a proton taken up upon Mn^{3+} reduction. This is also predicted based on the charges and bonding characters of the oxidized and reduced metal ions [17,57], and by computational studies of models of the FeSOD and MnSOD active sites [56,58]. Our data provide the first experimental demonstration of this essential coupling for MnSOD.

The fact that *any* protons are taken up demonstrates that some p*K*(s) are higher in Mn^{2+}SOD than in Mn^{3+}SOD. A higher p*K* is very reasonable for a group very close to the metal ion, which will experience a lower local positive electrostatic potential in the presence of Mn^{2+} than Mn^{3+}, and so will be more likely to protonate. The closer and more strongly coupled to Mn, the larger the effect and the more widely separated pK_{red}^{redox} and pK_{ox}^{redox}. However, once one group (the RCHA) has taken up a proton, that proton will restore the net charge of the active site to the value it had in the oxidized state. Thus all more distant groups will experience net electrostatically neutral uptake of an electron and a proton together, and their p*K*s are only expected to shift by relatively small amounts, due to different *distribution* of positive charge after reduction ($Mn^{2+}+H^+$) than before (Mn^{3+}). In this scenario, the RCHA is completely deprotonated in the oxidized state and completely protonated in the reduced state, $pK_{ox}^{redox} \ll pH$ and $pH \ll pK_{red}^{redox}$. The only pH dependence in $\Delta H^+/e^-$ that can be explained by the RCHA is a decrease in $\Delta H^+/e^-$ to less than 1 at high pH approaching pK_{red}^{redox} (when the reduced state would fail to bind an H^+) or low pH approaching pK_{ox}^{redox} (when the oxidized state would already be protonated). In between, the reduction potential would increase by 59 mV per pH unit decrease and $\Delta H^+/e^-$ would be constant at one.[5]

This behaviour is exemplified by the flat pH profile of proton uptake upon reduction obtained for FeSOD by Bull and Fee [9], indicating that either no other ionizable groups' p*K*s shift upon Fe^{3+} reduction or that any redox-sensitive p*K*s in the oxidized state are balanced by p*K*s of the same value in the reduced state [9]. Indeed, when a reduced-state p*K* was discovered, it was found to occur at pH 8.5 [24], as predicted based on the oxidized state p*K* of 8.6 [30].

Our data for MnSOD indicate that between pH values 8.6 and 11.1, more than one proton equivalent is taken up. This can be most simply explained by the existence of some additional ionization event occurring between pK_{ox}^{redox} and pK_{red}^{redox} that is shifted to higher pH in Mn^{2+}SOD than in Mn^{3+}SOD (pK_{ox}^{redox} and pK_{red}^{redox} must be very widely separated since $\Delta H^+/e^-$ is approximately 1 or greater in the range of MnSOD stability, so it is very reasonable that the active site should display other p*K*s in between). Moreover, it is also very reasonable that p*K*s should shift as a result of redistribution of charge upon metal ion reduction and proton uptake.

Eq. (5), corresponding to this model, adheres well to our data and yields $pK_{ox}=8.7$ and $pK_{red}=11.8$, for the oxidized and reduced states, respectively. These are in good agreement with Mn^{3+}SOD's p*K* of 8.5 or 9.7 for *E. coli* Mn^{3+}SOD [19,29] and Mn^{2+}SOD's p*K* of 10.5 [19] considering our relatively sparse data. Thus, the pH profile we observe is consistent with known ionization events, which are investigated in much greater detail elsewhere [18,19]. These p*K*s demonstrate the existence of additional groups competent to participate in proton transfer, whose more physiological p*K*s indicate that they will be predominantly protonated but that their protons will not be too costly to remove. The groups responsible for pK_{ox} and pK_{red} are thus important candidates for the immediate source of the second proton required for production of H_2O_2.

In the absence of measured pK^{redox} values, the RCHA can only be identified as a residue that is deprotonated in the oxidized state but protonated in the reduced state. The two most likely possibilities result in two alternate schemes for active site protonation (Schemes 2A,B). The more likely scenario on inorganic grounds is that the coordinated solvent is the RCHA (Scheme 2A), because this is the ionizable group whose ionizable proton is most intimately coupled to the metal ion. Moreover, for FeSOD, EXAFS and crystallographic data offer indirect experimental evidence that the existing solvent coordinated to Fe^{3+} is OH^- and therefore would be able to accept a proton upon metal ion reduction. However, this does not prove that it *does*, and Tyr34 remains an alternate candidate for the role until it can be shown that Tyr34 is already protonated at neutral pH in the oxidized state. We have now done just that, for both FeSOD and MnSOD, and so established experimentally that of the two most likely candidates, coordinated solvent is the RCHA, in agreement with calculations [56].

Thus, the FeSOD and MnSOD reactions can both be written

$$O_2^{\cdot -} + H^+ + P(M^{3+}OH^-) \rightarrow O_2 + P(M^{2+}H_2O) \quad (6a)$$

$$O_2^{\cdot -} + H^+ + P(M^{2+}H_2O) \rightarrow H_2O_2 + P(M^{3+}OH^-) \quad (6b)$$

where M is the Fe or Mn ion, P specifies the protein and protein-derived ligands but the coordinated solvent molecule is indicated explicitly as the RCHA, cycling between

[4] Gln146 is the MnSOD analog of Gln69 of FeSOD.

[5] Two or more residues spanning the pH range could collectively fulfil the same function if the p*K* of each member of the set simultaneously increases by Δp*K*.

OH^- and H_2O while the metal ion cycles between the +3 and +2 oxidation states.

It is interesting that the identity of the RCHA is the same in FeSOD and MnSOD, although the electronic structures of these two metal ions are significantly different from one another and change in different ways upon reduction. These distinctions appear to be over-ridden by the large electrostatic advantages of compensating locally for changes in the metal ion charge. For FeSOD, the fact that reduction is an electrostatically neutral process indicates that while the detailed distribution of charges in the active site may affect the reduction potential, the total charge of the protein and the average electrostatic potential at the active site will not affect the reduction potential. Instead, these can be varied independently of catalytic activity, for example to optimize binding to cellular targets [55].[6]

PCET is the rule in most biochemistry, where reductions commonly constitute gain of two H atoms or loss of an O atom. The best-known apparent exceptions are single electron-carrier proteins such as cytochromes and ferredoxins, although even here reduction is often accompanied by proton uptake [15,59–63]. SOD is a true enzyme that catalyzes formation of new bonds, and the tight coupling between the oxidation state of the metal ion and the protonation state of coordinated solvent (whose protons are only separated from the metal ion by two bonds) produces a built-in source of an H^+ to go with the electron transferred [29], in addition to a device for tuning the reduction potential [34,35]. Many other metalloenzymes that mediate redox chemistry also bind and release H^+ in the reaction. For example, in Cu,ZnSOD, the bridging His ligand dissociates from Cu when Cu^{2+} is reduced to Cu^{1+}, and takes up an H^+ ($pK \approx 10.8$) [64–66]. 'This' H^+ is then available to protonate $O_2^{\cdot -}$ in conjunction with its reduction, as Cu^{1+} is reoxidized to Cu^{2+} and rebinds the His [67]. Nitrogenase catalyzes reduction of N_2 and $8H^+$ to $2NH_3$ and H_2 [68,69] and the successive reductions of the MoFe protein are proposed to be accompanied by protonation [70], including protonation of ligands to nitrogenase's metal cluster [71] and even the clusters themselves [72]. Thus, coupling of H^+ transfer to electron transfer is crucial in redox-active enzymes in general and the identity of the RCHA is a central element of the mechanism. SOD's highly efficient system of using the coordinated solvent requires that a coordination site be devoted to this role, but results in an exceptionally tightly coupled self-contained PCET site. The independence of this mechanism from ligating or surrounding amino acids may reflect SOD's potentially primitive origin [73] and presents this enzyme as a case in which the protein may aid in substrate binding, restrict and fine tune activity, but the reactivity resides completely in the inorganic metal site.

[6]For the case of MnSOD, the additional proton gained upon reduction at high pH results in a counter-intuitive predicted raising of the reduction potential by a more negative average electrostatic potential in the active site above pH 8.6.

6. Conclusions

We have shown that MnSOD takes up a proton upon reduction. This provides important direct experimental support for the prevalent assumption that key features of MnSOD's mechanism are the same as those of FeSOD. We have used ^{13}C NMR spectroscopy to directly observe Tyr34 at the position closest to the phenolic OH and identify Tyr34's protonation state at neutral pH in each of Fe^{2+}SOD, Fe^{3+}SOD and Mn^{3+}SOD. Our finding that in both Fe^{3+}SOD and Mn^{3+}SOD, Tyr34 is protonated at neutral pH, is not surprising. However, it provides previously lacking experimental evidence that Tyr34 cannot be the group that accepts a proton upon SOD reduction, and thus that the redox-coupled proton acceptor must instead be coordinated solvent. We find that for MnSOD the stoichiometry of proton uptake upon reduction rises to greater than 1, and approaches 2, at pH values above 8. This indicates that at least one more active site residue can take up and release protons in the physiological range, and could serve as the source of the second proton required for production of H_2O_2. The p*K*s resulting from the pH dependence of redox-coupled proton uptake agree well with those observed spectroscopically.

7. Abbreviations

DT	dithionite
DSS	4,4-dimethyl-4-silapentane sodium sulfonate
MES	morpholinoethanesulfonic acid
PCET	proton-coupled electron transfer
RCHA	redox-coupled proton acceptor
SOD	superoxide dismutase

Acknowledgements

AFM gratefully acknowledges funding from the N.S.F. (0129599) and the N.I.H. (GM55210-03) and T.C. Brunold for careful reading of the manuscript.

References

[1] A.-F. Miller, D.L. Sorkin, Comments Mol. Cell. Biophys. 9 (1) (1997) 1–48.
[2] I. Fridovich, Protein Sci. 7 (12) (1998) 2688–2690.
[3] I. Fridovich, J. Biol. Chem. 272 (30) (1997) 18515–18517.
[4] F. Lavelle, M.E. McAdam, E.M. Fielden, P.B. Roberts, K. Puget, A.M. Michelson, Biochem. J. 161 (1977) 3–11.
[5] W.C. Barrette Jr., D.T. Sawyer, J.A. Fee, K. Asada, Biochemistry 22 (1983) 624–627.

[6] A.-F. Miller, in: K. Wieghardt et al. (Ed.), Handbook of Metalloproteins, Wiley, Chichester, UK, 2001, pp. 668–682.
[7] L.L. Ingraham, D.L. Meyer, in: E. Frieden (Ed.), Biochemistry of the Elements, Plenum, New York, 1985.
[8] D.T. Sawyer, Oxygen Chemistry, Oxford University Press, 1991.
[9] C. Bull, J.A. Fee, J. Am. Chem. Soc. 107 (1985) 3295–3304.
[10] C. Bull, E.C. Niederhoffer, T. Yoshida, J.A. Fee, J. Am. Chem. Soc. 113 (1991) 4069–4076.
[11] J.P. Roth, J.C. Yoder, T.-J. Won, J.M. Mayer, Science 294 (2001) 2524–2526.
[12] C. Tommos, G.T. Babcock, Biochim. Biophys. Acta Bioenerg. 1458 (2000) 199–219.
[13] S.P. Rafferty, J.G. Guillemette, A.M. Berghuis, G.D.B.M. Smith, A.G. Mauk, Biochemistry 35 (1996) 10784–10792.
[14] G.R. Moore, G.W. Pettigrew, R.C. Pitt, R.J.P. Williams, Biochim. Biophys. Acta 590 (1980) 261–271.
[15] F.A. Leitch, G.R. Moore, G.W. Pettigrew, Biochemistry 23 (1984) 1831–1838.
[16] W.C. Stallings, A.L. Metzger, K.A. Pattridge, J.A. Fee, M.L. Ludwig, Free Radic. Res. Commun. 12–13 (1991) 259–268.
[17] C.F. Baes Jr., R.E. Mesmer, The Hydrolysis of Cations, Wiley, 1976.
[18] T.A. Jackson, J. Xie, E. Yikilmaz, A.-F. Miller, T.C. Brunold, J. Am. Chem. Soc. 124 (2002) 10833–10845.
[19] J. Maliekal, A. Karapetian, C. Vance, E. Yikilmaz, Q. Wu, T. Jackson, T.C. Brunold, T.G. Spiro, A.-F. Miller, J. Am. Chem. Soc. 124 (2002) 15064–15075.
[20] M.E. McAdam, F. Lavelle, R.A. Fox, E.M. Fielden, Biochem. J. 165 (1977) 81–87.
[21] M. Pick, J. Rabani, F. Yost, I. Fridovich, J. Am. Chem. Soc. 96 (23) (1974) 7329–7333.
[22] M.S. Lah, M.M. Dixon, K.A. Pattridge, W.C. Stallings, J.A. Fee, M.L. Ludwig, Biochemistry 34 (1995) 1646–1660.
[23] E.C. Niederhoffer, J.A. Fee, V. Papaefthymiou, E. Münck, in: Isotope and Nuclear Chemistry Division, Annual report, Los Alamos National Laboratory, 1987, pp. 79–84.
[24] D.L. Sorkin, A.-F. Miller, Biochemistry 36 (16) (1997) 4916–4924.
[25] D.L. Sorkin, D.K. Duong, A.-F. Miller, Biochemistry 36 (1997) 8202–8208.
[26] J.V. Bannister, W.H. Bannister, G. Rotilio, CRC Crit. Rev. Biochem. 22 (2) (1987) 111–180.
[27] A. Terech, J. Pucheault, C. Ferradini, Biochem. Biophys. Res. Commun. 113 (1983) 114–120.
[28] T. Hunter, K. Ikebukuro, W.H. Bannister, J.V. Bannister, G.J. Hunter, Biochemistry 36 (16) (1997) 4925–4933.
[29] M.M. Whittaker, J.W. Whittaker, Biochemistry 36 (1997) 8923–8931.
[30] J.A. Fee, G.J. McClune, A.C. Lees, R. Zidovetzki, I. Pecht, Isr. J. Chem. 21 (1981) 54–58.
[31] D.L. Tierney, J.A. Fee, M.L. Ludwig, J.E. Penner-Hahn, Biochemistry 34 (1995) 1661–1668.
[32] M. Schmidt, Eur. J. Biochem. 262 (1999) 117–126.
[33] A. Carlioz, D. Touati, EMBO J. 5 (1986) 623–630.
[34] A.L. Schwartz, E. Yikilmaz, C.K. Vance, S. Vathyam, R.L. Koder Jr., A.-F. Miller, J. Inorg. Biochem. 80 (2000) 247–256.
[35] C.K. Vance, A.-F. Miller, J. Am. Chem. Soc. 120 (3) (1998) 461–467.
[36] C.K. Vance, A.-F. Miller, Biochemistry 37 (1998) 5518–5527.
[37] T.O. Slykhouse, J.A. Fee, J. Biol. Chem. 251 (1976) 5472–5477.
[38] J.M. McCord, I. Fridovich, J. Biol. Chem. 244 (1969) 6049–6055.
[39] W.F. Beyer Jr., I. Fridovich, Biochemistry 26 (1987) 1251–1257.
[40] H.W. Kim, J.A. Perez, S.J. Ferguson, I.D. Campbell, FEBS Lett. 272 (12) (1990) 34–36.
[41] J.W. Whittaker, M.M. Whittaker, J. Am. Chem. Soc. 113 (1991) 5528–5540.
[42] J.-L. Hsu, Y. Hsieh, C. Tu, D. O'Connor, H.S. Nick, D.N. Silverman, J. Biol. Chem. 271 (30) (1996) 17687–17691.
[43] D.L. Rabenstein, S. Fan, Anal. Chem. 58 (1986) 3178–3184.
[44] A.A. Valcour, R.C. Woodworth, J. Magn. Reson. 66 (1986) 536–541.
[45] G. Otting, B.A. Messerle, L.P. Soler, J. Am. Chem. Soc. 118 (1996) 5096–5102.
[46] A.J. Shaka, J. Keeler, R. Freeman, J. Magn. Res. 53 (1983) 313–340.
[47] R.J. Ogg, P.B. Kingsley, J.S. Taylor, J. Magn. Reson. B 104 (1994) 1.
[48] S.H. Smallcombe, S.L. Patt, P.A. Keiger, J. Magn. Reson. A 117 (1995) 295.
[49] T. Inubishi, E.T. Becker, J. Magn. Reson. 51 (1983) 128–133.
[50] B.-H. Oh, J.L. Markley, Biochemistry 29 (1990) 4012–4017.
[51] N.U. Jain, T.C. Pochapsky, Biochem. Biophys. Res. Commun. 258 (1) (1999) 54–59.
[52] L. Bertini, C. Luchinat, NMR of Paramagnetic Molecules in Biological Systems. Benjamin/Cummings, Menlo Park, CA, 1986.
[53] G.N. LaMar, W.D. Horrocks Jr., R.H. Holm, NMR of Paramagnetic Molecules, Academic Press, New York, 1973.
[54] http://www.bmrb.wisc.edu/ref_info/statsel.htm
[55] R.A. Edwards, H.M. Baker, G.B. Jameson, M.M. Whittaker, J.W. Whittaker, E.N. Baker, J. Biol. Inorg. Chem. 3 (1998) 161–171.
[56] W.G. Han, T. Lovell, L. Noodleman, Inorg. Chem. 41 (2) (2002) 205–218.
[57] J. Li, C.L. Fisher, J.-L. Chen, D. Bashford, L. Noodleman, Inorg. Chem. 35 (1996) 4694–4702.
[58] C.L. Fisher, J.-L. Chen, J. Li, D. Bashford, L. Noodleman, J. Phys. Chem. 100 (1996) 13498–13505.
[59] D.G. Nettesheim, T.E. Meyer, B.A. Feinberg, J.D. Otvos, J. Biol. Chem. 258 (1983) 8235–8239.
[60] N.K. Rogers, G.R. Moore, FEBS Lett. 228 (1988) 69–73.
[61] P.D. Barker, A.G. Mauk, J. Am. Chem. Soc. 114 (1992) 3619–3624.
[62] B. Shen, L.L. Martin, J.N. Butt, F.A. Armstrong, C.D. Stout, G.M. Jensen, P.J. Stephens, G.N. LaMar, C.M. Gorst, B.K. Burgess, J. Biol. Chem. 268 (1993) 25928–25939.
[63] J. Hirst, J.L.C. Duff, G.N.L. Jameson, M.A. Kemper, B.K. Burgess, F.A. Armstrong, J. Am. Chem. Soc. 120 (1998) 7085–7094.
[64] J.A. Fee, P.E. DiCorleto, Biochemistry 12 (1973) 4893–4899.
[65] L. Bertini, C. Luchinat, J. Am. Chem. Soc. 107 (1985) 2178–2179.
[66] H.A. Azab, L. Banci, M. Borsari, C. Luchinat, M. Sola, M.S. Viezzoli, Inorg. Chem. 31 (1992) 4649–4655.
[67] J.A. Tainer, E.D. Getzoff, K.M. Beem, K.S. Richardson, D.C. Richardson, J. Mol. Biol. 160 (1982) 181–217.
[68] W.H. Orme-Johnson, Annu. Rev. Biophys. Biophys. Chem. 14 (1985) 419–459.
[69] B.K. Burgess, Chem. Rev. 90 (1990) 1377–1406.
[70] R.N.F. Thorneley, D. Lowe, in: T.G. Spiro (Ed.), Molybdenum Enzymes, Wiley–Interscience, New York, 1985.
[71] J.W. Peters, M.H.B. Stowell, S.M. Soltis, M.G. Finnegan, M.K. Johnson, D.C. Rees, Biochemistry 36 (6) (1997) 1181–1187.
[72] T. Lovell, J. Li, D.A. Case, L. Noodleman, J. Am. Chem. Soc. 124 (2002) 4546–4547.
[73] P. Joshi, P.P. Dennis, J. Bacteriol. 175 (1993) 1572–1579.
[74] J. Cavanagh, W.J. Fairbrother, A.G. Palmer III, N.J. Skelton, Protein NMR Spectroscopy, Principles and Practice, 1st Edition, Academic Press, 1996.
[75] http://www.idtdna.com/program/faqs/faqs.asp
[76] G.E.O. Borgstahl, M. Pokross, R. Chehab, A. Sekher, E.H. Snell, J. Mol. Biol. 296 (2000) 951–959.